Isothermal annealing of selenium (Se)-implanted silicon carbide: Structural evolution and migration behavior of implanted Se

Z.A.Y. Abdalla[1], E. G. Njoroge[1, 2], M. Mlambo[3], S.V. Motloung[4, 5], J.B. Malherbe[1], T.T. Hlatshwayo[1]

[1]Department of Physics, University of Pretoria, Pretoria 0002, South Africa

[2]ENGAGE, University of Pretoria, Pretoria 0002, South Africa[3]Institute for [3]Nanotechnology and Water Sustainability, College of Science, Engineering and Technology, University of South Africa, Florida Science Campus, 1710, South Africa

[4]Department of Chemical and Physical Sciences, Walter Sisulu University, Private Bag ×1, Mthatha, South Africa

[5]Department of Physics, Sefako Makgatho Health Sciences University, P.O. Box 94, Medunsa, 0204, South Africa

HIGHLIGHTS

- Polycrystalline SiC substrates were implanted with Se ions of 200 keV at RT, 350 °C and 600 °C.
- Implantation at RT amorphized SiC while implantation at 350 and 600 °C retained crystallinity with defects.
- The samples were subjected to an isothermal annealing process at 1300 °C, 1350 °C and 1400 °C up to 80 h.
- Diffusion of the Se implanted into SiC was only observed in the RT samples.

ABSTRACT

Isothermal annealing studies of selenium-implanted silicon carbide (SiC) were conducted at temperatures >1200 ºC. Implantation were performed using Se ions of 200 keV to a fluence of 1×10^{16} cm^{-2}at room temperature, 350 °C and 600 °C. After implantations, samples were then subjected to an isothermal annealing process at 1300 ºC, 1350 ºC and 1400 ºC for 10 hours cycles up to 80 hours. The radiation damage in SiC and its morphological change were characterized using Raman spectroscopy and scanning electron microscopy (SEM), respectively. The migration of implanted Se was monitored by Rutherford backscattering spectrometry (RBS). Implantation at RT amorphized SiC while implantation at 350 and 600 ºC retained crystallinity with defects. Isothermal annealing led to significant recrystallization during the first annealing cycle in all

annealing temperatures. The broadening of the Se RBS profile was observed in the RT implanted samples only during the first and second annealing cycles at all annealing temperatures. The diffusion coefficients at 1300 ºC, 1350 ºC and 1400 ºC were estimated to be 1.4 $\times 10^{-20}$ m^2s^{-1}, 2 $\times 10^{-20}$ m^2s^{-1} and 2.5 $\times 10^{-20}$ m^2s^{-1}, respectively, which yielded to an activation and pre-exponential factor of 2 $\times 10^{-22}$ J and 1.7 $\times 10^{-16}$ m^2s^{-1} respectively. No measurable diffusion of the Se implanted into SiC was observed in the isothermally annealed hot implanted samples (at implantation temperature of 350 °C and 600 °C) confirming the radiation enhanced migration of Se in the RT implanted samples.

Keywords: *Ion implantation; Polycrystalline SiC; Isothermal annealing; Diffusion*

1. INTRODUCTION

The success of the very high temperature gas cooled reactors (VHTGRs) like a pebble bed modular reactor (PBMR) depends greatly on the retainment of fission products. In the PBMR the retainment is achieved by coating the fuel kernel. The fuel kernel, which contains the nuclear fuel (UO_2) is coated with a porous carbon buffer layer, an inner pyrolytic carbon (IPyC) layer, a silicon carbide (SiC) layer and (3) an outer pyrolytic carbon (OPyC) layer [1,2]. Of these coating layers, SiC is the main barrier of fission products. The coated particle is known as Tristructural isotropic (TRISO).

Some of the VHTGRs have an outlet temperature of 900 °C [3]. Moreover, the TRISO fuel particles are exposed to temperatures that exceed 900 °C [4]. SiC has the ability to maintain most of its properties at high temperatures of about 1700 °C in vacuum [4,5]. Hence, its function is not only a diffusion barrier for fission products, but also provides structural integrity to the coated fuel particle. In general, the SiC coating layer of TRISO particles is a structural element that ensures the fission products are contained, and thus forms the safety rationale for the nuclear reactor. To get more insight into the retainment of different radioactive fission products, the migration behavior of fission products in SiC need to be investigated.

In recent years, the migration of fission products in different polytypes of SiC has been extensively studied using ion implantation. In this process, ions are accelerated and made to penetrate a solid target, which leads to a change in the surface physical and chemical properties of the material. A great number of research studies have been performed by our group at the University of Pretoria.

These studies resulted in numerous publications that have reviewed the diffusion of important fission products in SiC such as silver, cesium, xenon, krypton, iodine, and strontium [4,6-10]. ^{79}Se is one of the hazardous fission products that is found in high-level radioactive waste created by the reprocessing of spent nuclear fuel from the operation of nuclear reactors, as well as in spent fuel reprocessing facilities [11]. It is a β-emitter, and the unacceptable risks posed by the presence of Se is the increased likelihood of inducing cancer [12]. Therefore, its migration in SiC need to be investigated. Quite recently the migration behavior of Se in SiC was investigated. The substrate temperature during ion implantation was (RT) [11] and higher temperatures of 350 and 600 ºC [12] was investigated. In these previous studies the implanted samples were sequentially annealed from 1000 ºC to 1500 ºC in steps of 100 ºC for 10 hour. Room temperature implantation formed an amorphous upper layer of SiC. Hot implantation retained the crystal structure of SiC, but caused some structural changes and radiation damage. In the RT implanted sample, diffusion of Se towards the surface began at 1300 °C. No measurable diffusion was observed in the hot implanted samples after sequential annealing up to 1500 °C. In the sequential annealing experiments, the annealed samples have different amount of radiation damage owing to healing that occurred during annealing at lower temperatures. The aim of current study is to obtain information on the role of defects/radiation damage in the transport properties of selenium through polycrystalline SiC. For this purpose, some polycrystalline SiC samples implanted under the same conditions were isothermally annealed at temperatures ≥ 1300 °C.

2. EXPERIMENTAL PROCEDURE

In this work, polycrystalline SiC wafers obtained from Valley Design Corporation were used. These wafers consisted of mainly columnar crystallites, a few micrometers in diameter, well aligned along the growth direction, with smaller crystals not parallel to the columns as well [13]. SiC wafers were composed of mainly 3C-SiC polytype with some hexagonal polytype (6H-SiC). A fluence of 1×10^{16} cm^{-2} selenium ions of 200 keV were implanted into the wafers at RT, 350 °C and 600 °C under vacuum of about 10^{-4} Pa. The flux was kept below 10^{13} cm^{-2}s^{-1} during implantation to minimize radiation induced heating. Ion beam homogeneity over the samples surfaces was achieved by the use of 2dimensional beam scanning. The implantations were done at the Friedrich-Schiller-University Jena, Germany. To investigate the role of defects/radiation

damage in the migration behavior of selenium (Se) implanted into polycrystalline SiC, some of the implanted samples were isothermally annealed at 1300 °C, 1350 °C and 1400 °C for 10 h cycles up to 80 h under vacuum (10^{-4} Pa). Annealing was performed using a computer-controlled Webb 77 graphite furnace.

The selenium-implanted silicon carbide samples were analysed using Rutherford backscattering spectrometry (RBS) after each annealing cycle. The samples were analysed with He+ particles of 1.6 MeV. The backscattered particles were detected by silicon surface barrier detector through 165°, with a beam current of about 15 nA during the measurements. To achieve high accuracy and reduce noise in measurement, 3 repeated measurements were collected for each individual charge of 8 μC and the results were averaged. The energy in channel number in the RBS Se profile was converted into depth using Ziegler, Biersack and Littmark (ZBL) stopping powers [14], and density of SiC (3.21 g cm^{-3}). Se profiles in the depth scale were fitted to a Gaussian function to obtain the range straggling (ΔR_p) and projected ranges (R_p) [15]. The surface morphology before and after each annealing cycle was monitored by field emission scanning electron microscopy (FEG-SEM) using a Zeiss Ultra 55 with an in-lens detector at 2 kV. The SiC microstructure pre- and post-isothermal annealing was examined using a T64000 Raman triple grating spectrometer system (from HORIBA scientific) from Jobin Yvon (JY) Technology. Raman measurements were obtained using a laser excitation wavelength in the visible region of 514.5 nm. An Olympus microscope with a 50 × objective lens was used to focus the light to a spot size of ~2 μm^2.

3. RESULTS AND DISCUSSION

3.1 ROOM TEMPERATURE IMPLANTATION

Our previous studies showed that Se ions implanted at room temperature lead to the disappearance of the signal intensities/features of Raman spectra of pristine SiC, indicating amorphization of implanted SiC [11]. In this study, the defects were monitored using the longitudinal optical (LO) Raman mode [16]. The measurement of structural recovery and recrystallization was based on the change in peak position and full width at half maximum (FWHM) of the LO mode as a function of temperature.

In the current study, the effect of isothermal treatment on the LO mode of SiC annealed at 1300 °C, 1350 °C and 1400 °C was investigated. This was done by annealing the implanted samples for 10 h cycles up to 80 h (80 h at 1350 °C is not shown here). Fig. 1 shows the LO peak intensity as a function of time for RT implanted SiC isothermally annealed at different temperatures. As the annealing duration increased, the LO mode became more intense, indicating a decrease in defects or damage concentration in the implanted SiC [17,18]. This also indicates an increase in the number of scattering molecules irradiated by the incident laser, which means that the crystals have grown in size [17,19]. From Fig. 1 it is also evident that the intensity of the samples annealed at 1400 °C for 10 h is lower than those of samples annealed at 1300 °C and 1350 °C for 10 h. This shows that the amount or crystal size distribution is lower in the former due to the presence of pores and cavities [20], as will be discussed later in the SEM results.

The structural evolution of SiC was quantified by calculating the FWHM of the LO mode. Fig. 2 shows the FWHM of the LO mode as a function of temperature. The FWHM of the sample annealed at 1300 °C for 10 h is approximately 12 cm^{-1}, it is then decreased to 11 cm^{-1} after annealing at same temperature for the second annealing cycle (20 h). The narrowing of the FWHM is an indication of the recrystallization i.e. the presence of defects of any kind will shorten the phonon lifetime and thus broaden the linewidth [17,21]. Therefore, the crystalline material gives sharper Raman line than the amorphous material. No significant changes were observed after subsequent annealing cycles up to 80 hours. A FWHM of about 11 cm^{-1} was observed in both samples annealed at 1350 °C and 1400 °C for 10 h. This is narrower than that one of 1300 °C indicating a higher degree of crystallization. The fact that the structural order improves with temperature can be confirmed by low FWHM value of 10 cm^{-1} at 1400 °C during the final annealing cycle (80 h)

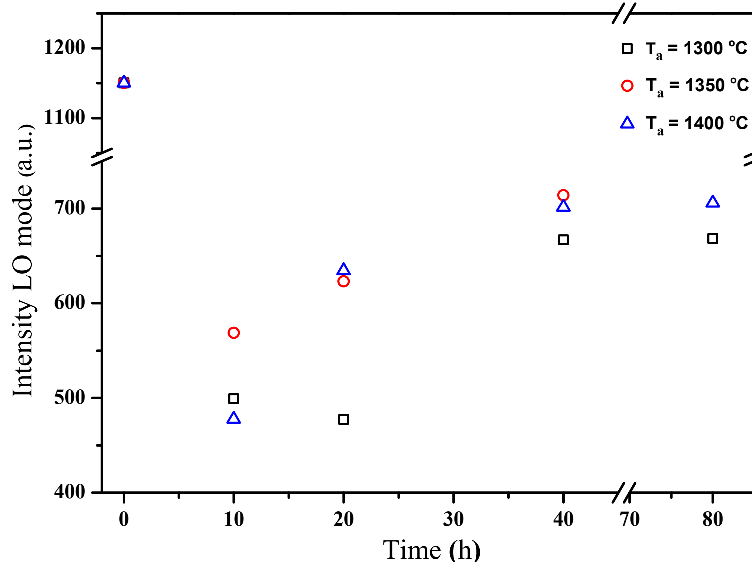

Fig. 1: *The intensity of LO mode of SiC implanted with Se at room temperature as a function of time during isothermal annealing at 1300, 1350 and 1400 °C.*

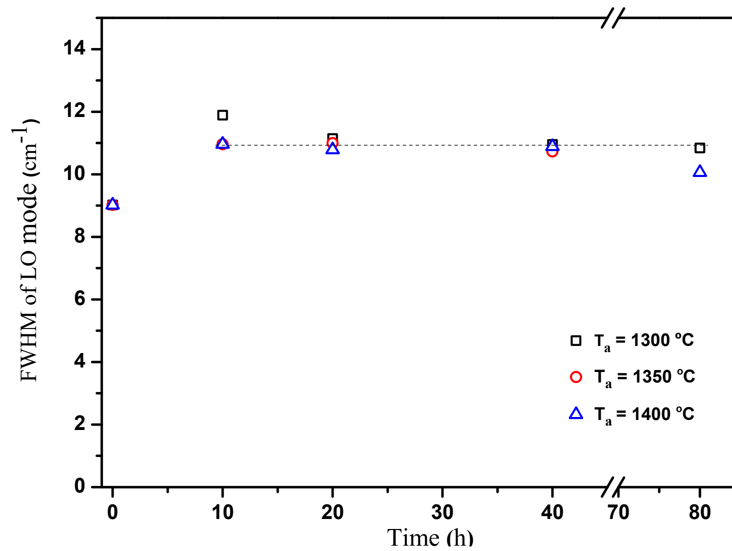

Fig. 2: *The FWHM of LO mode of SiC implanted with Se at room temperature as a function of time during isothermal annealing at 1300, 1350 and 1400 °C.*

The LO mode position as a function of time after isothermal annealing at different temperatures is shown in Fig. 3. In all annealed samples, the first annealing cycle shifted the LO mode to about 965.4 cm^{-1}, which is at higher wavenumber compared to the pristine SiC LO mode (964.7 cm^{-1}). This indicates the presence of the compressive in SiC due to the change in the bond distances between the atoms. Shifting to higher wavenumber is usually an indication of decreased length of

chemical bonds, relative to their length in the unstressed crystals [22]. This stress resulted from the implanted ions causing damage to the crystal lattice [23]. There was no considerable change in the LO position during the second annealing cycle (20 h) in the sample annealed at 1300 °C, whereas in the samples annealed at 1350 °C and 1400 °C, the LO mode shifted by 0.5 cm^{-1} to higher wavenumbers, indicating greater compressive stress. In all temperatures, the LO mode shifted to approximately 966 cm^{-1} after annealing for 40 h. No further shift was observed in the sample annealed at 1300 °C during the final annealing cycle (80 h), while isothermal annealing at 1350 °C and 1400 °C caused further shift to higher wavenumbers.

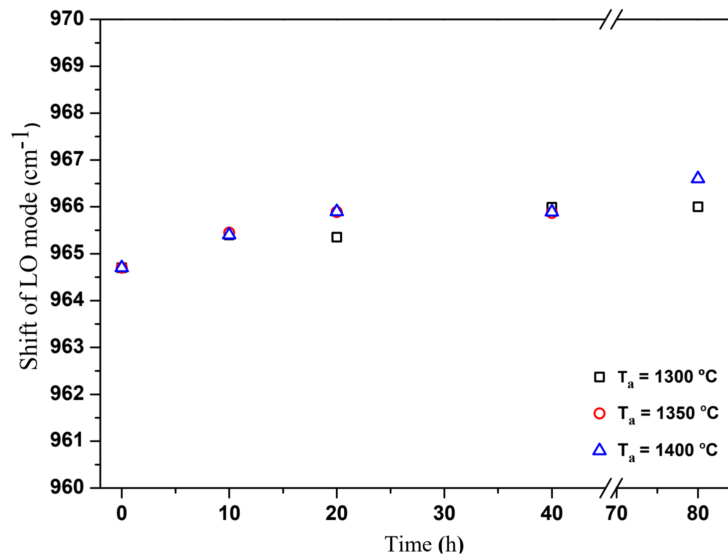

Fig. 3: *The Raman shift of LO mode of SiC implanted with Se at room temperature as a function of time during isothermal annealing at 1300, 1350 and 1400 ºC.*

The effects of annealing on the surface morphology of the implanted samples were monitored using a scanning electron microscopy (SEM). The SEM micrographs of the room temperature implanted samples before and after isothermal annealing at 1300, 1350 and 1400 ºC are shown in Fig. 4, 5 and 6 respectively. The SEM micrographs showed that the surface features are clear and more distinguishable at higher annealing temperatures. In Fig. 4 (a), a SEM image of the RT implanted sample annealed at 1300 °C for 10 h shows a surface consisting of small crystals and regions devoid of features indicating recrystallization. However, the featureless regions suggest the presence of defects. No significant morphological changes were observed after subsequent annealing up to 80 h (Fig. 4 (b)). Annealing of RT implanted sample at 1350 °C for 10 h resulted

in distinguishable features on the surface with visible crystals as can be seen in Fig. 5 (a). The crystals became more prominent with few pores after subsequent annealing cycles (Fig. 5 (b)). The SEM micrograph showed more prominent crystals, pores and cavities after annealing at 1400 °C for 10 h (Fig.6 (a)) compared to the sample annealed at 1300 ºC in Fig. 5 (a). Subsequent annealing cycles resulted in slight growth of the surface crystals (Fig. 6 (b)). These SEM observations confirm the fact that surface development and the crystals growth are greatly affected by temperature. The results are in good agreement with the measured FWHM of Raman spectra (LO mode).

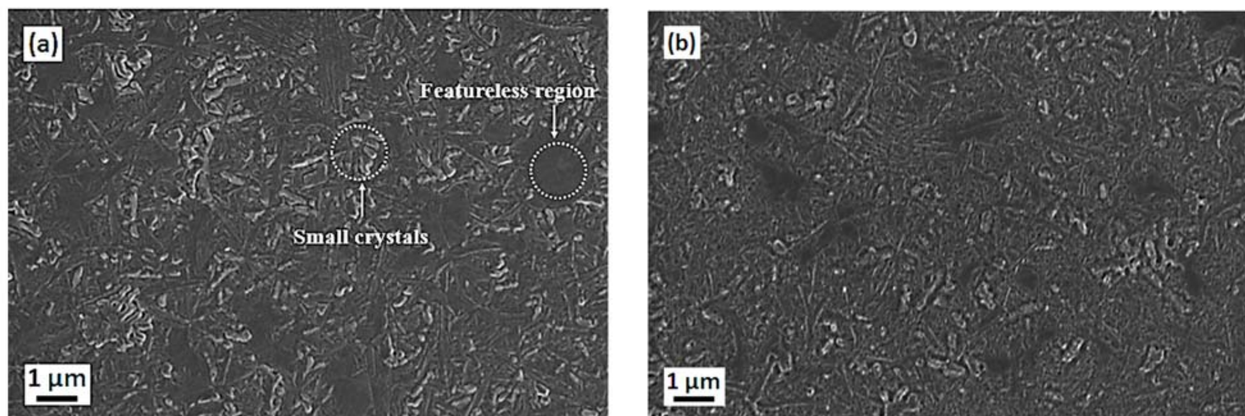

Fig. 4*: SEM micrographs of room temperature selenium implanted SiC surfaces after vacuum annealing at 1300 °C for (a) 10 h and (b) 80 h.*

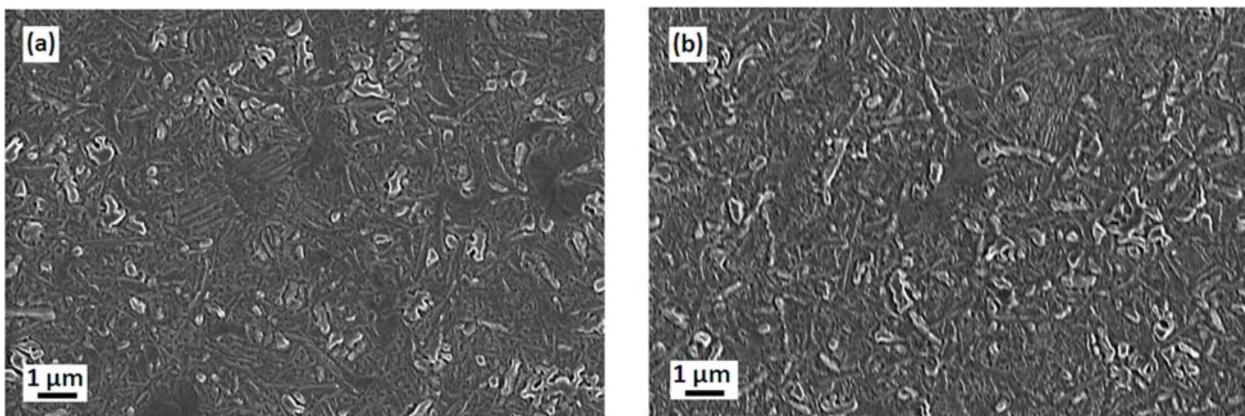

Fig. 5: SEM micrographs of room temperature selenium implanted SiC surfaces after vacuum annealing at 1350 °C for (a) 10 h and (b) 80 h.

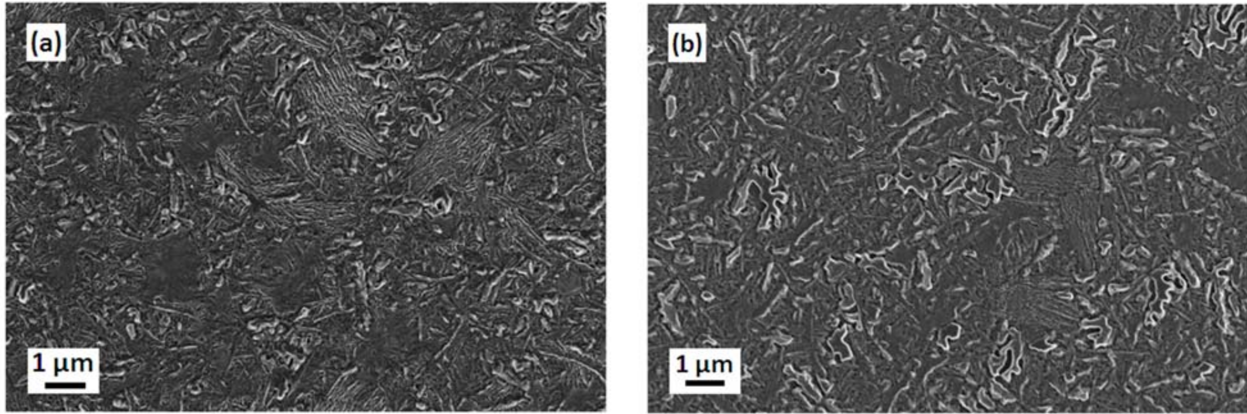

Fig. 6: SEM micrographs of room temperature selenium implanted SiC surfaces after vacuum annealing at 1400 °C for (a) 10 h and (b) 80 h.

The migration behavior of Se implanted into SiC was investigated using Rutherford backscattering spectroscopy (RBS). The RBS spectra of samples isothermally annealed at different temperatures are shown in Fig. 7. The arrows in Fig. 7 (a) indicate the surface position of Se, Si and C. The squares full width half maximum (FWHM) and the retained ratio of Se as functions of annealing time are shown in Fig. 8 and 9, respectively. Annealing the RT implanted sample at 1300 °C for 10 h caused the Se profile to shift towards the surface (Fig. 7 (a)) accompanied by peak broadening and 10% loss of implanted Se from the surface (Fig. 8 and Fig. 9). These observations/results indicate that the diffusion of implanted Se was towards the surface. Further annealing at same temperature for 20 h resulted in a rather reduced broadening compared to the 10 h annealed sample accompanied by a slight loss of implanted Se. No broadening was further observed after subsequent annealing cycles up to 80 h at 1300 ºC. In the final cycle (80 h), the loss of implanted Se was approximately 20%.

Annealing the RT sample at 1350 °C for 10 h led to a significant increase in peak broadening, compared to that obtained at 1300 °C for 10 h (Fig. 8). This broadening was accompanied by a loss of approximately 15%. A rather reduced width broadening occurred up to the third annealing cycle. Whereas, no noticeable broadening occurred during the final annealing cycle (80 h). The fact that the measured width remain constant after the third annealing cycle indicates that the amorphous state resulting from implantation, which allows selenium diffusion, is no longer

present. Therefore, Se only diffused in the highly defective of amorphous SiC. The Se profiles of 1350 °C have similar broadening as the profiles of the sample isothermal annealed at 1400 °C (Fig. 8), but significant loss of selenium from the surface is observed after the first annealing cycle (Fig. 9). In the final cycle (80 h), losses were approximately 25% and 40% at 1350 °C and 1400 °C respectively.

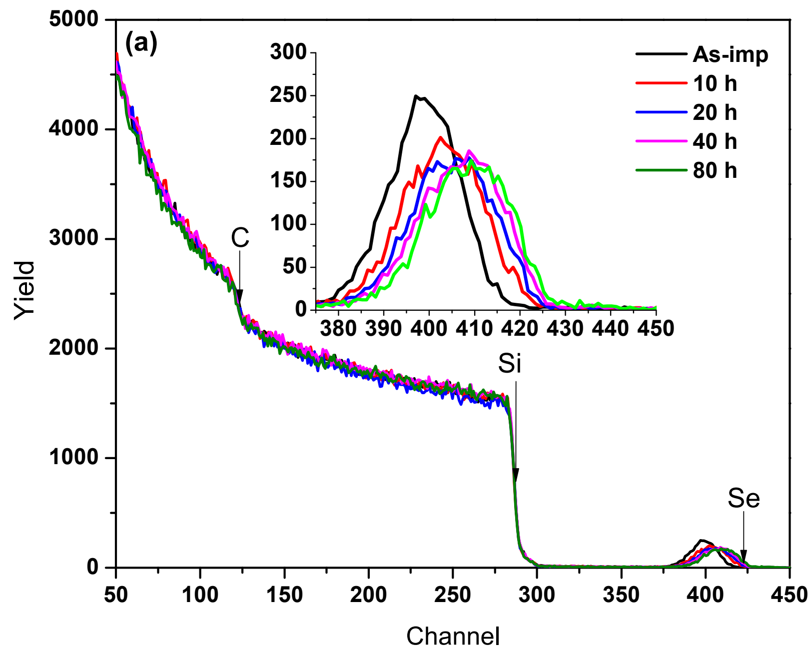

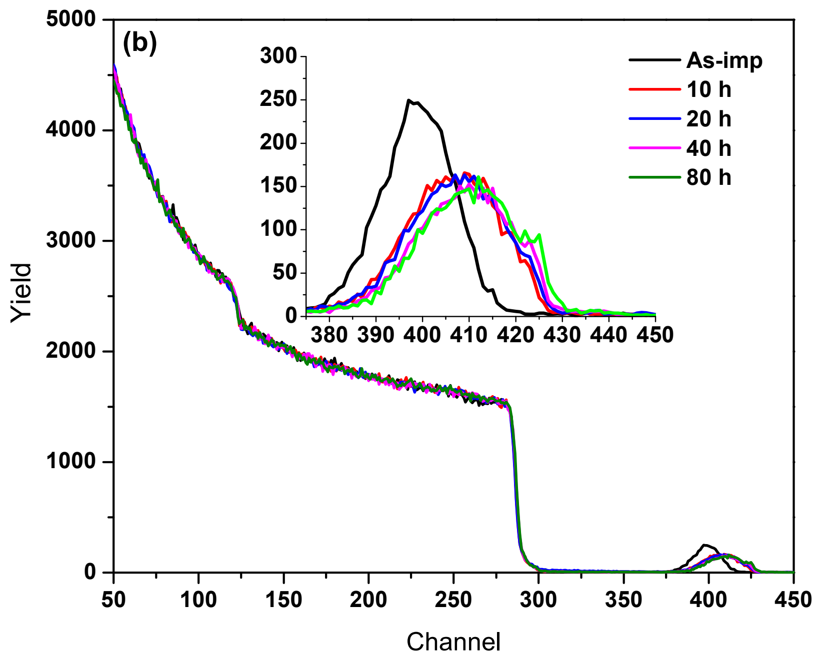

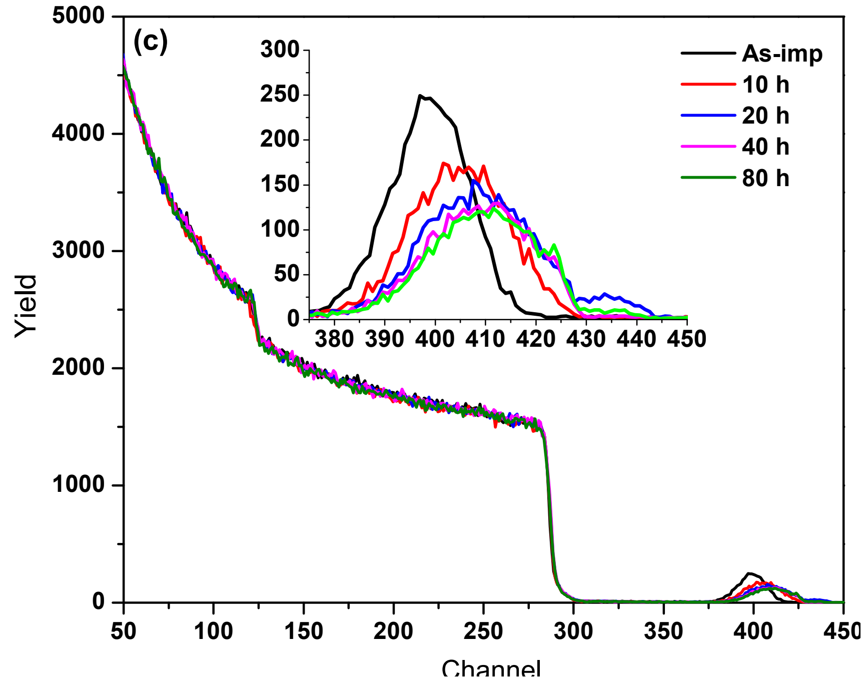

Fig. 7: *RBS spectra of Se implanted into polycrystalline SiC at RT and after isothermal annealing at 1300 °C, 1350 °C and 1400 °C.*

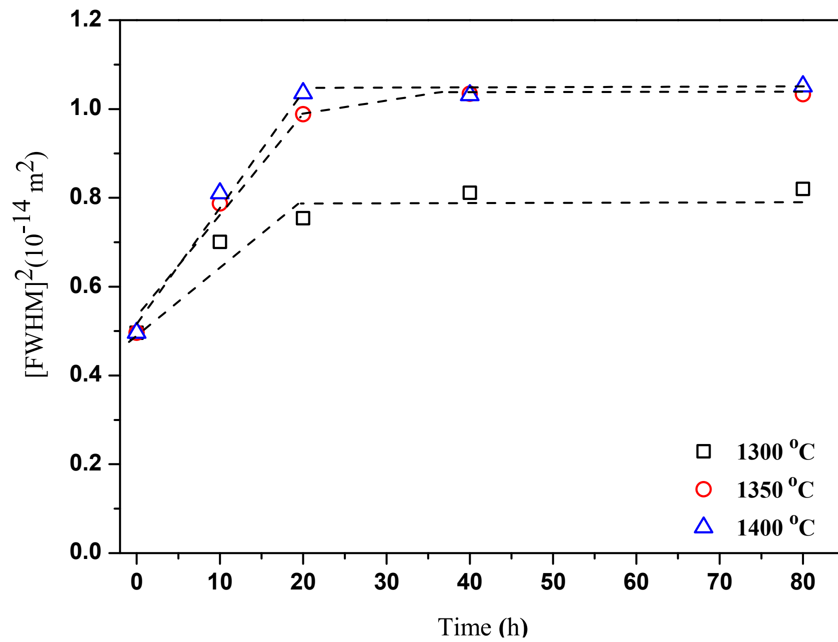

Fig. 8: *Isothermal annealing curves of RT implanted samples at 1300 °C, 1350 °C and 1400 °C.*

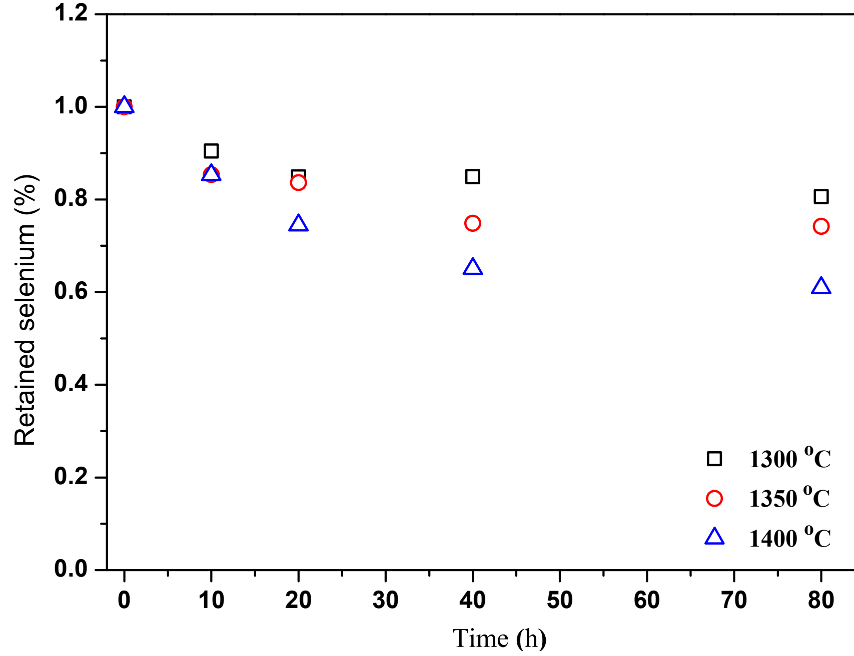

Fig. 9: *The ratio of retained Se in polycrystalline SiC at RT after isothermal annealing at 1300 °C, 1350 °C and 1400 °C.*

Since the Se peak broadening during the first annealing cycle is due to diffusion of Se in the highly defective/amorphous SiC, the diffusion coefficient (D) of Se in highly defective or amorphous SiC was estimated from the broadening of the FWHM of selenium profiles after annealing according to [24]:

$$[W(t)]^2 = 4Dt\ln(2) + [W(0)]^2$$

Where W(0) and W(t) are the FWHM of the as-implanted and annealed samples respectively. The diffusion coefficients at 1300, 1350 and 1400 °C were found to be 1.4×10^{-20} m^2s^{-1}, 2×10^{-20} m^2s^{-1} and 2.5×10^{-20} m^2s^{-1}, respectively. The dependence of diffusion coefficient on temperature is generally expressed by the Arrhenius equation as:

$$\ln D = -\frac{E_a}{k_B}\frac{1}{T} + \ln D_o$$

Where k_B is the Boltzmann's constant, E_a is the activation energy, T is the annealing temperature and D_o is pre-exponential factor. The activation energy of selenium diffusion in amorphous silicon

carbide can be determined from the slope of the ln D versus the inverse of the temperature graph. E_a and D_o were found to be 2 $\times 10^{-22}$ J/mol and 1.7 $\times 10^{-16}$ m^2s^{-1}, respectively. No previous diffusion coefficients of Se in SiC were found in literature hence the obtained activation energy and pre-exponential factor were not compared with any literature values.

3.2 HIGH TEMPERATURE IMPLANTATION

Implantation of Se ions at 350 ºC and 600 ºC retained crystallinity of SiC with more defects in the 350 ºC implanted samples compared to 600 °C [11]. The effect of isothermal annealing on the LO mode of SiC at 1300 ° C, 1350 °C and 1400 °C was investigated. This was also done by annealing the implanted samples for 10 h cycles up to 80 h. Fig. 10 shows the LO intensity as a function of annealing temperature in both the hot implanted annealed samples. The intensities were 248.2 and 329.5 a. u for samples implanted at 350 °C and 600 °C, respectively. Isothermal annealing at 1300 °C caused general increase in the intensity of LO mode with increasing annealing cycles up 80 h in both hot implanted samples indicating the progressive healing of defects. Annealing of implanted samples at 1350°C increased the intensity of LO mode during the first annealing cycle. Fig. 10 (b) shows that the LO mode of 600 °C is more intense in this cycle as compared to 350 °C. For the 350 °C implanted samples, a slight increase in intensity was observed during the second annealing cycle and no change was observed for any further annealing cycles up 80 h. No change in LO mode intensity of the 600 °C implanted sample was observed after the first annealing cycle. Annealing of implanted samples at 1400 °C for 10 h increased the intensity of the LO mode to positions close to that of 1350 °C. The intensity increased slightly during subsequent annealing cycles up to 80 h in both samples. The overall results demonstrate the intensity increases with time up to a value that depends on temperature. This indicates the gradual annealing of defects with annealing temperatures and time.

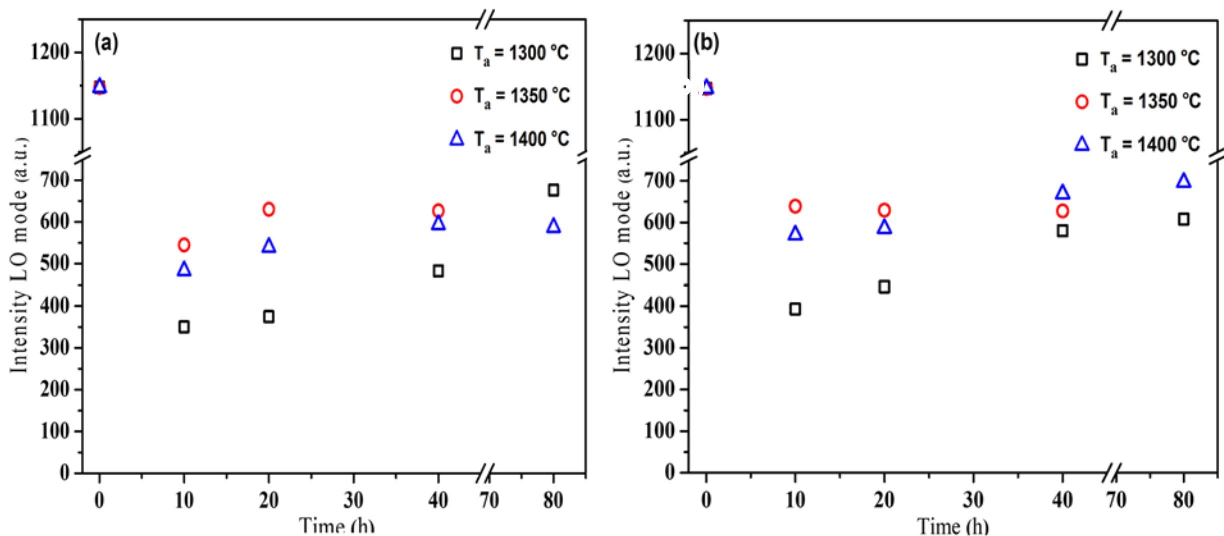

Fig. 10: *The LO mode intensity of SiC implanted at (a) 350 °C and (b) 600 °C as a function of time during isothermal annealing at 1300 °C, 1350 °C and 1400 °C.*

Fig. 11 shows the full width at half maximum (FWHM) of the LO mode as a function of temperature. The FWHM of LO mode obtained from 350 °C and 600 °C implanted samples are 12.1 cm^{-1} and 11.96 cm^{-1}, respectively (not shown in Fig. 11). These values are broader in comparison with the virgin sample (9.6 cm^{-1}). In both implanted samples, at all annealing temperatures, the FWHM decreased to approximately 11.5 cm^{-1} during the first annealing cycle as can be seen in Fig. 11 (a) and (b). This indicates an increase in the degree of crystallinity. No considerable changes were observed after subsequent annealing cycles from 10 h to 80 h.

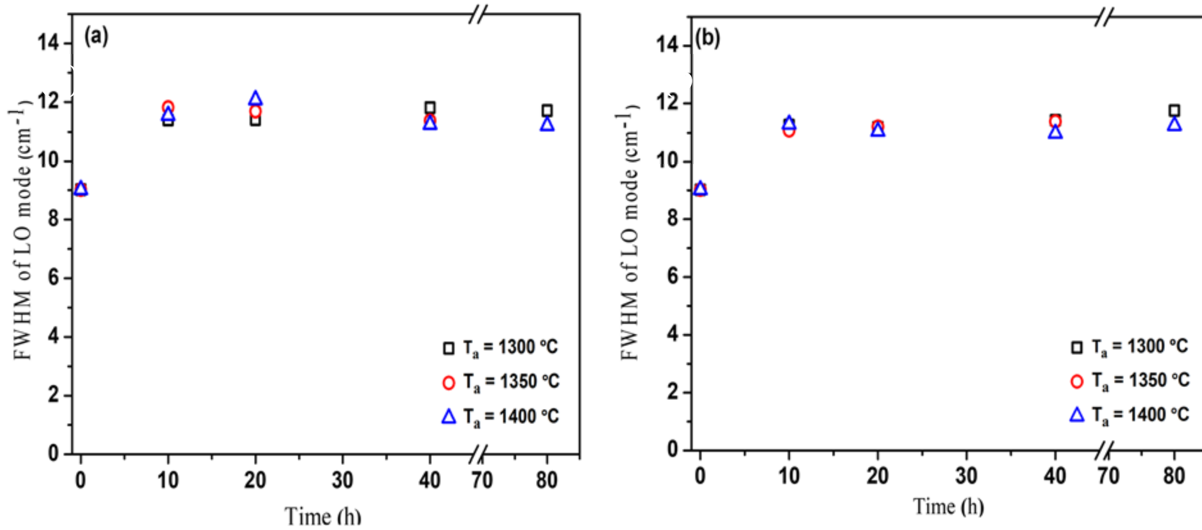

Fig. 11: *The FWHM of LO mode of SiC implanted at (a) 350 °C and (b) 600 °C as a function of time during isothermal annealing at 1300 °C, 1350 °C and 1400 °C.*

Fig. 12 shows the LO mode position as a function of time during isothermal annealing at different temperatures. In Fig. 12 (a) it is quite evident that the annealing of 350 °C implanted samples at 1300 °C and 1350 °C resulted in the appearance of the LO mode at approximately 965.5 cm^{-1} during the first annealing cycle, slightly higher than the pristine sample (964.7 cm^{-1}. This is attributed to the presence of the compressive stress in bonds between atoms as a result of a change in atomic distances. Whereas in the 350 °C sample annealed at 1400 °C, the LO mode appeared at 965 cm^{-1}, suggesting less compressive stress compared to those of 1300 °C and 1350 °C . Only slight changes in the LO mode position were observed during the subsequent annealing cycles up to 80 h at these temperatures. The shift to higher wavenumbers increased slightly to 966.3 cm^{-1} during the final 80 h cycle. In the case of the 600 °C implanted samples, Fig. 12 (b), annealing for 10 h resulted in the appearance of the LO mode at approximately 965.7 cm^{-1} at all temperatures. No change in LO position was observed during the subsequent annealing cycles up to 80 h. It is noticeable that all implanted samples (RT, 350 °C and 600 °C) experience approximately equal stress during the first annealing cycle at all temperatures.

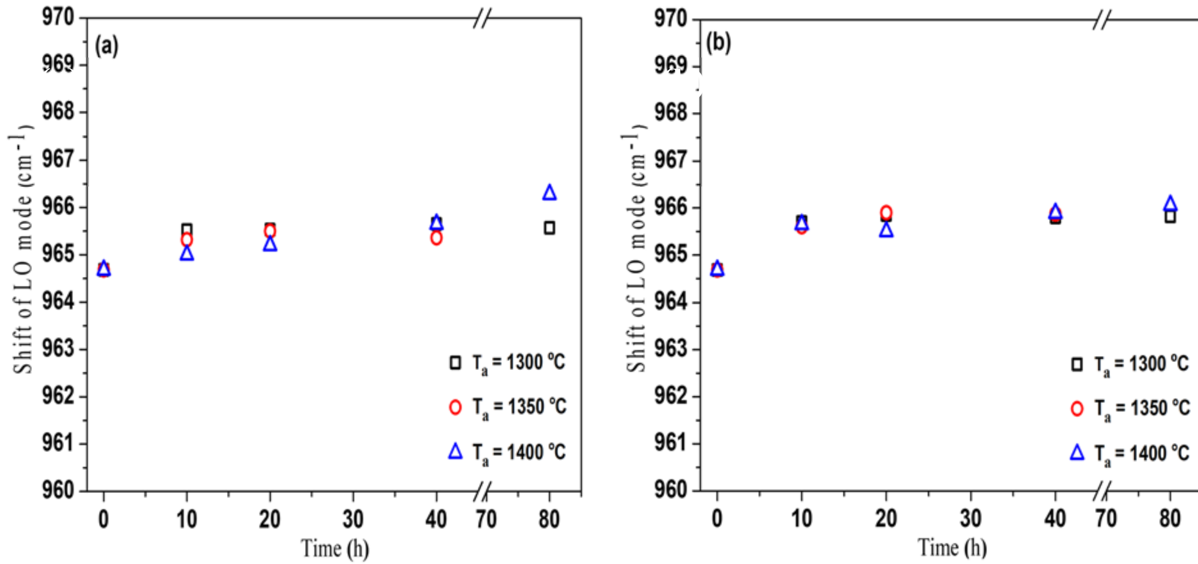

Fig. 12: The Raman shift of LO mode of SiC implanted with Se at (a) 350 °C and (b) 600 °C as a function of time during isothermal annealing at 1300 °C, 1350 °C and 1400 °C.

SEM micrographs of the 350 °C and 600 °C Se implanted samples are shown in Fig. 13. Implantation at 350 °C reduced the polishing marks with grains still visible (Fig. 13 (a)) indicating the presence of a crystalline structure. This (350 °C) is approximately the critical temperature at which no amorphization in SiC can occur [12,25]. No significant change was observed on the 600 °C implanted surface (Fig. 13 (b)) compared to the pristine (not shown). This is due to the fact that 600 ºC is well above the critical amorphization temperature.

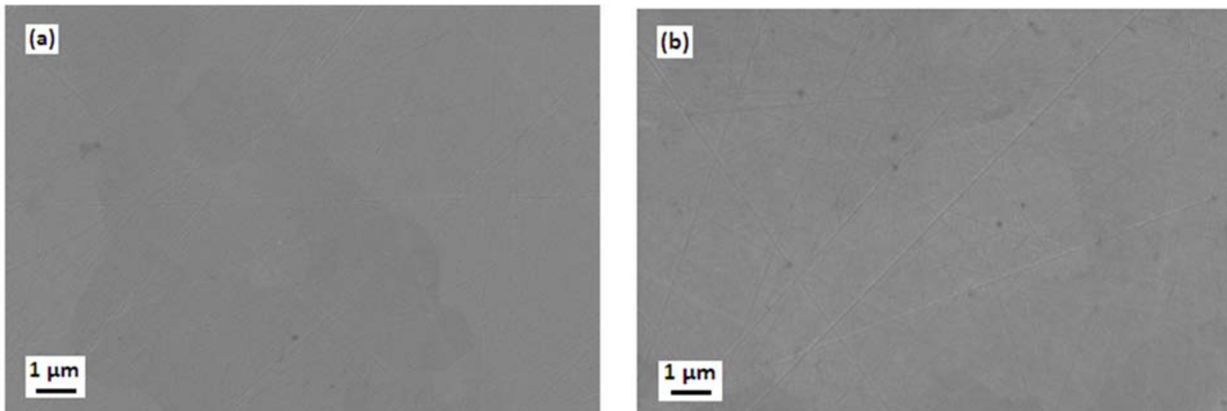

Fig. 13: SEM micrographs of polycrystalline SiC implanted with Se at (a) 350 °C and (b) 600 °C.

The isothermal annealing of both hot implanted samples resulted in grains appearing on the surfaces. Some opening of grain boundaries were also observed with few open pores on these boundaries (see Fig. 14 and Fig. 15). This is due to thermal etching that is more preferred on the grai boundaries where they are lose atoms. The influence of different defects in both samples was not observed in this study.

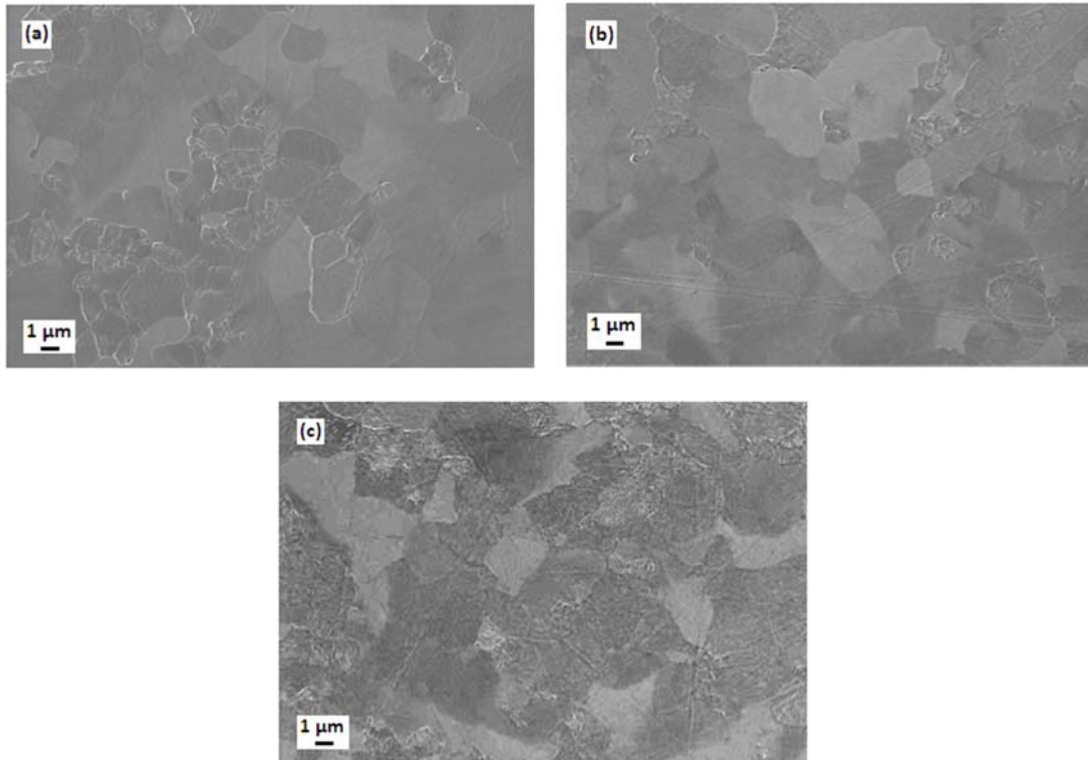

Fig. 14: *SEM micrographs of polycrystalline SiC implanted with Se at 350 °C after annealing at (a) 1300 °C, (b) 1350 °C and (c) 1400 °C for 40 h.*

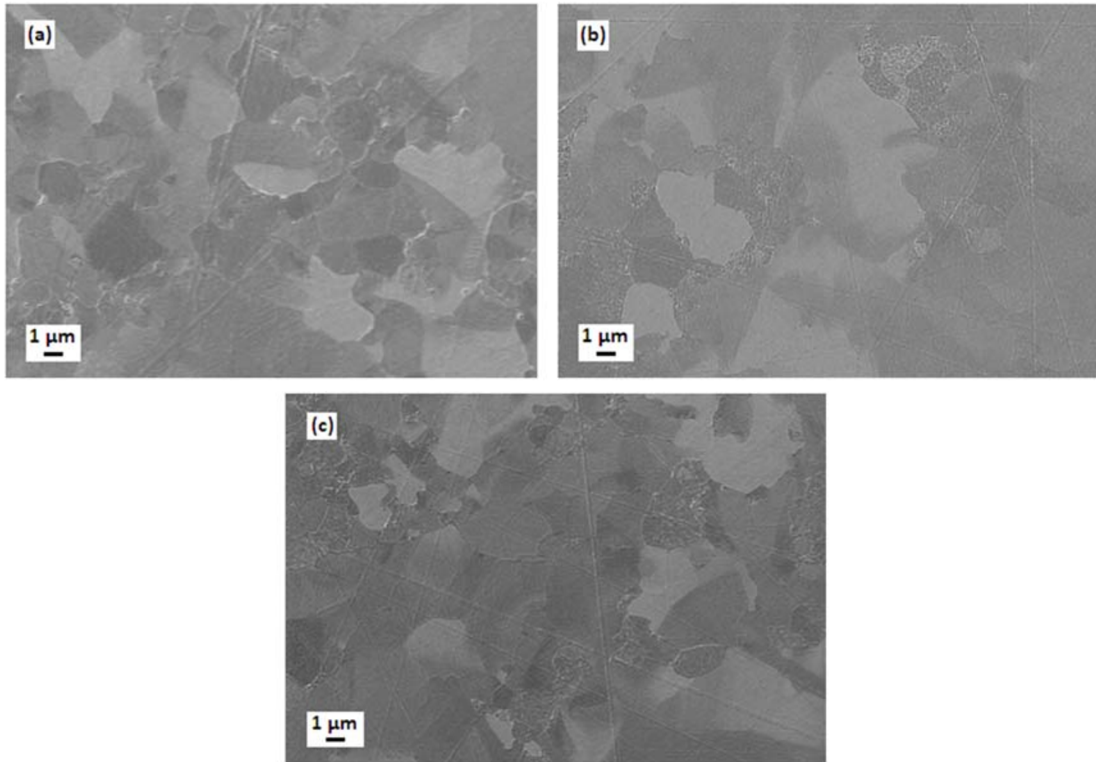

Fig. 15: *SEM micrographs of polycrystalline SiC implanted with Se at 600 °C after annealing at (a) 1300 °C, (b) 1350 °C and (c) 1400 °C for 40 h.*

The RBS spectra of the hot implanted samples obtained before and after annealing are shown in Fig. 16 and 17. The squares of the FWHM (of Se depth profiles) after isothermal annealing are shown in Fig. 18 while the retained ratio as a function of annealing temperature is shown in Fig. 19. Annealing of the both hot implanted samples at 1300 ºC, 1350 ºC and 1400 ºC for 10 h, resulted in some shift of implanted Se towards the surface. This was accompanied by neither broadening nor loss of implanted Se indicating lack of diffusion in these samples. Further annealing at the same temperatures up to 80 h caused no detectable changes in all temperatures. These results point to the initial radiation damage as the driving force of the shift after the 10 h annealing cycles. Before, the first annealing cycles, hot implanted samples have more defects compare to the samples annealed for 10 h. During the 10 h annealing cycles the initial defects are enough to allow the migration or shift of implanted Se towards the surface without diffusion. The samples annealed for 10 h have less defects which are not enough for migration of Se to occur during further annealing up to 80 h.

Annealing of RT samples resulting in a strong diffusion towards the surface accompanied by loss after the first annealing cycle at all temperatures and annealing of the both hot implanted samples resulting in the shift of implanted Se after the first annealing cycle in all temperatures. This confirm the role of radiation damage in the transport properties of implanted Se. The as-implanted RT samples are initially highly defective or amorphous while the hot implanted samples have less defects. Hence, Se only diffuses in the highly defective SiC in all annealing temperatures in this study. In nuclear reactor environment SiC will be exposed to different irradiation including ions of energy of about 100 MeV in the presence of He (from nuclear reactions (n,α)) at elevated temperatures. Even though the current results are positive for nuclear reactor, to get more insight, the role of swift heavy ions and He in the migration of Se will be investigated.

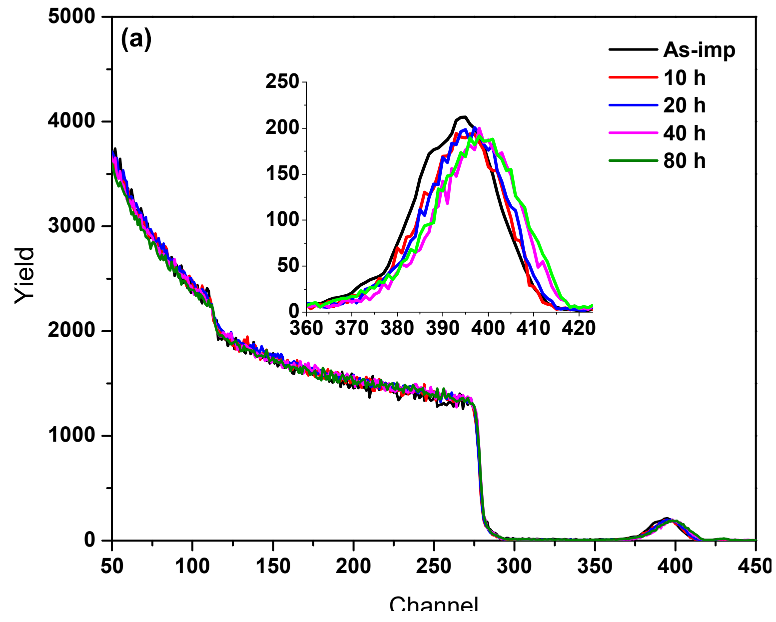
(a)
As-imp
10 h
20 h
40 h
80 h
Yield
Channel

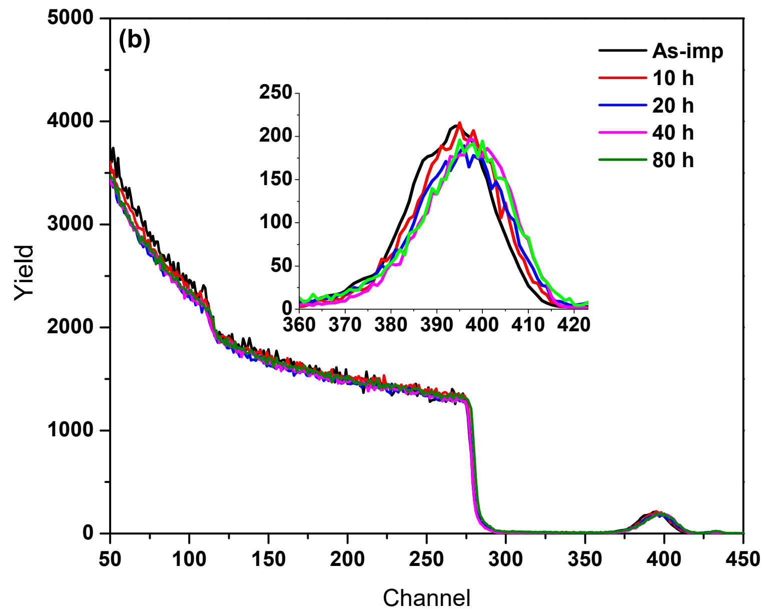
(b)
As-imp
10 h
20 h
40 h
80 h
Yield
Channel

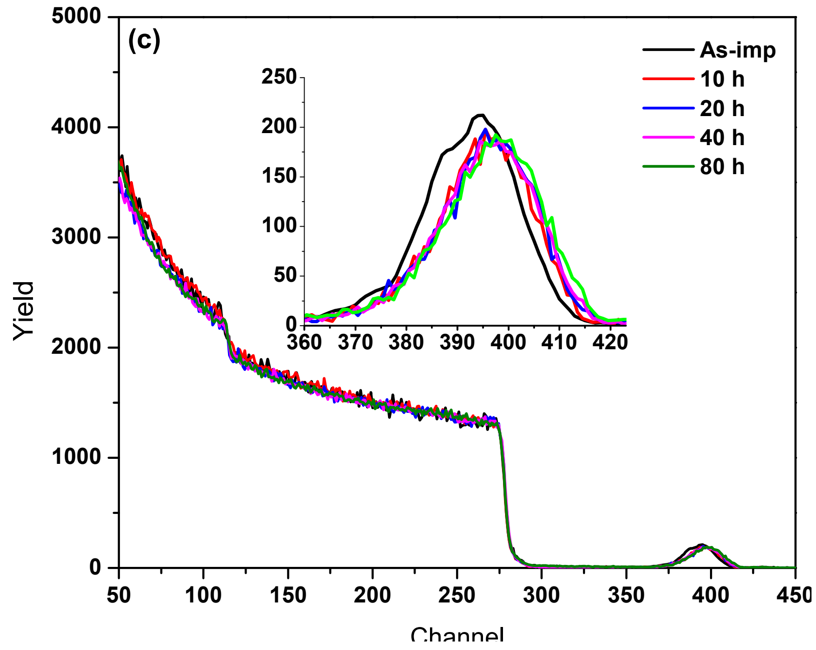

Fig. 16: *RBS spectra of Se implanted into polycrystalline SiC at 350 °C and after isothermal annealing at 1300 °C, 1350 °C and 1400 °C.*

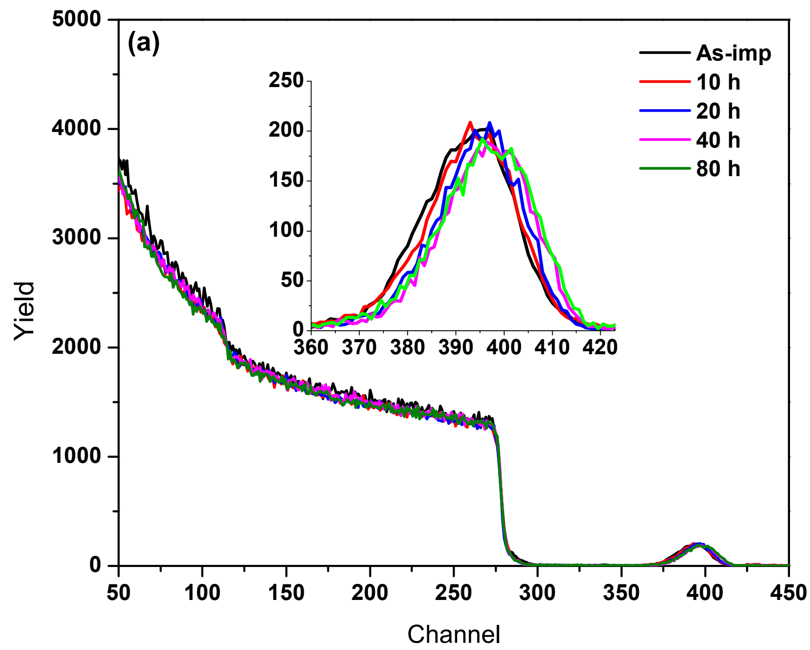

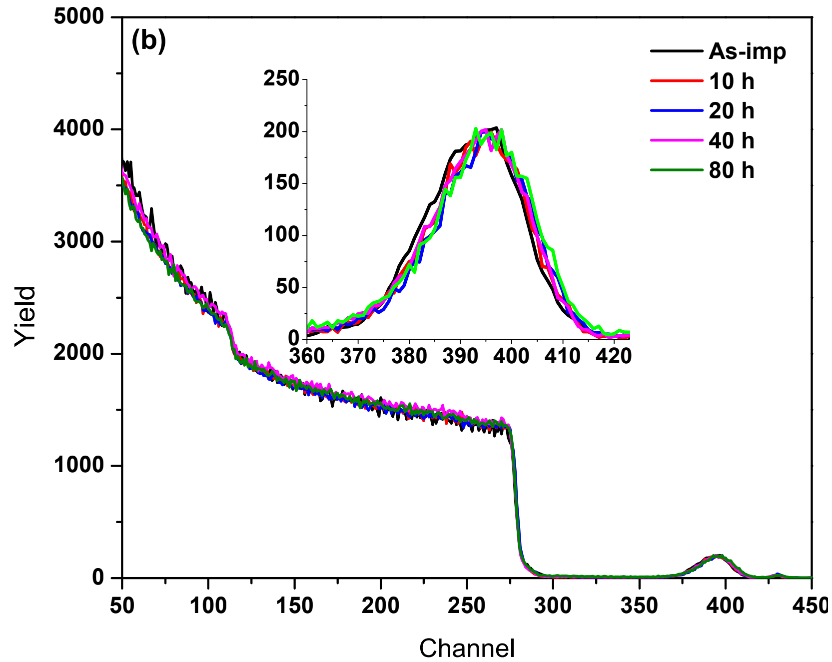

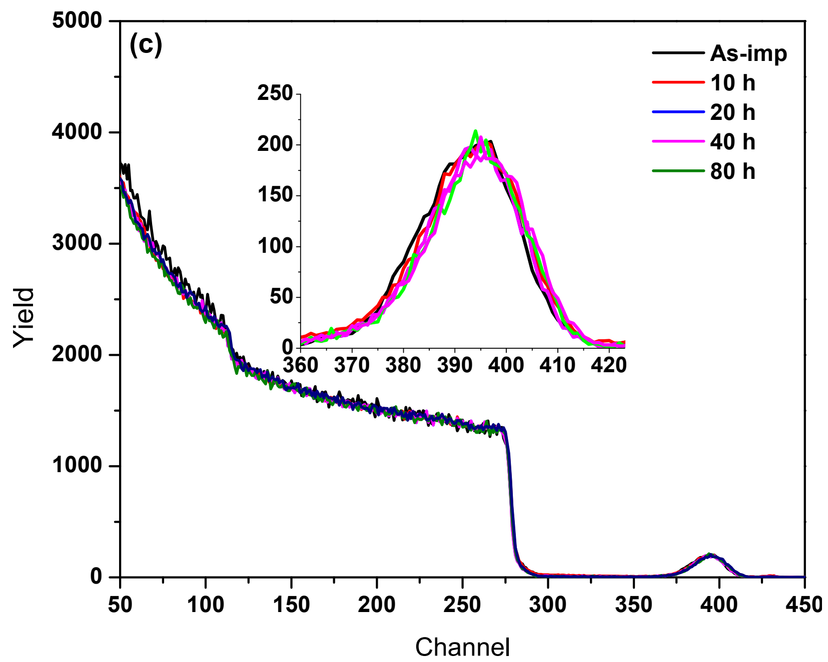

***Fig. 17**: RBS spectra of Se implanted into polycrystalline SiC at 600 °C and after isothermal annealing at 1300 °C, 1350 °C and 1400 °C.*

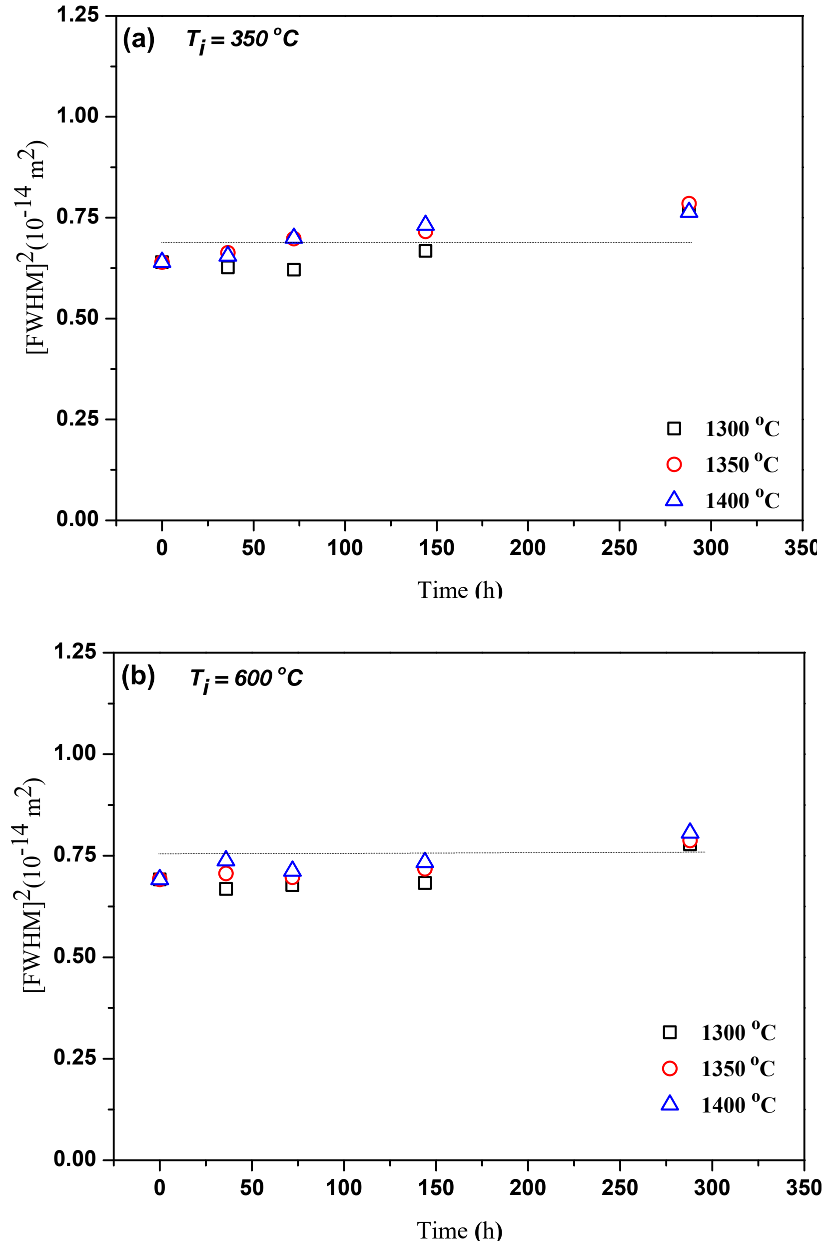

Fig. 18: *Isothermal annealing curves of (a) 350 °C and (b) 600 °C implanted samples at 1300 °C, 1350 °C and 1400 °C.*

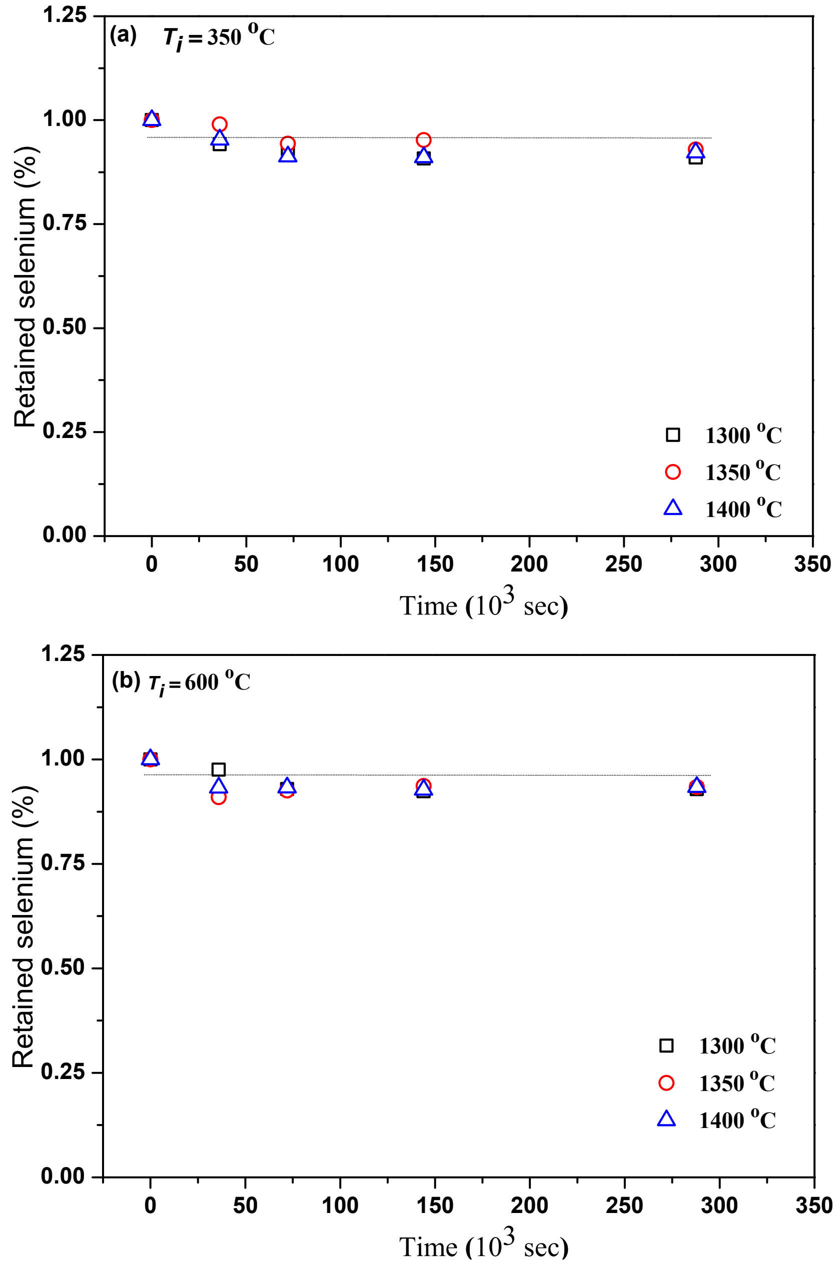

Fig. 19: *The ratio of retained Se in polycrystalline SiC at (b) 350 °C and (b) 600 °C after isothermal annealing.*

4. CONCLUSION

The effect of isothermal annealing on the migration behavior of implanted of 200 keV selenium implanted into polycrystalline SiC at RT, 350 °C and 600 °C was investigated. The RBS spectra showed that annealing of the RT implanted samples caused the broadening of the Se profiles towards the surface of the SiC substrate. Diffusion coefficients estimated from the RT implanted

samples were 1.4 $\times10^{-20}$ m^2s^{-1}, 2 $\times10^{-20}$ m^2s^{-1} and 2.5 $\times10^{-20}$ m^2s^{-1} at 1300 ºC, 1350 ºC and 1400 °C, respectively with an activation energy of 2 $\times10^{-22}$ J and a pre-exponential factor of 1.7 $\times10^{-16}$ m^2s^{-1}. In comparison, heat treatment of hot implanted samples (350 °C and 600 °C) resulted in no measurable diffusion of implanted Se further pointing to radiation enhanced migration of Se. This indicates that Se only diffuses in the highly defective of amorphous SiC. The Raman results showed a decrease in damage concentration with annealing cycles, as well as the presence of compressive stress in the RT implanted SiC. SEM observations confirmed the fact that crystal growth and surface morphology development are severely influenced by temperature. The results of this study indicate the suitability of polycrystalline SiC as a diffusion barrier for selenium.

ACKNOWLEDGEMENT

Financial support received from the National Research Foundation (NRF), South Africa and The World Academy of Science (TWAS) is gratefully acknowledged.

REFERENCES

[1] O. Ö Gülol, Ü. Çolak, and B. Yıldırım, Performance analysis of TRISO coated fuel particles with kernel migration, J. Nucl. Mater. 374 (1–2) (2008) 168–177.

[2] W.F. Skerjanc, J.T. Maki, B.P. Collin, D.A. Petti, Evaluation of design parameters for TRISO-coated fuel particles to establish manufacturing critical limits using PARFUME, J. Nucl. Mater. 469 (2016) 99–105.

[3] J.B. Malherbe, E. Friedland, N.G. Van Der Berg, Ion beam analysis of materials in the PBMR reactor, Nucl. Instrum. Methods Phys. Res., Sect. B 266 (8) (2008) 1373–1377.

[4] J.B. Malherbe, Diffusion of fission products and radiation damage in SiC, J. Phys. D. Appl. Phys. 46 (47) (2013) 1–52.

[5] N.G. van der Berg, J.B. Malherbe, A.J. Botha, E. Friedland, Thermal etching of SiC, Appl. Surf. Sci 258 (2012) 5561–5566.

[6] E. Friedland, N. G. Van Der Berg, T. T Hlatshwayo, R. J. Kuhudzai, J. B. Malherbe, E. Wendler, and W. Wesch, Diffusion behavior of cesium in silicon carbide at T> 1000° C, Nucl. Instrum. Methods Phys. Res., Sect. B 286 (2012) 102–107.

[7] E. Friedland, K. Gärtner, T. T. Hlatshwayo, N. G. Van Der Berg, and T. T. Thabethe, Influence of radiation damage on xenon diffusion in silicon carbide, Nucl. Instrum. Methods Phys. Res., Sect. B 332 (2012) 415–420.

[8] E. Friedland, N. G. van der Berg, J. B. Malherbe, E. Wendler, and W. Wesch, Influence of radiation damage on strontium and iodine diffusion in silicon carbide, J. Nucl. Mater. 425 (2012) 205–210.

[9] E. Friedland, T. Hlatshwayo, N. van der Berg, Influence of radiation damage on diffusion of fission products in silicon carbide, Phys. Status Solidi 10 (2) (2013) 208–215.

[10] T. T. Hlatshwayo, J. H. O'Connell, V. A. Skuratov, M. Msimanga, R. J. Kuhudzai E. G. Njoroge, and J. B. Malherbe, Effect of Xe ion (167 MeV) irradiation on polycrystalline SiC implanted with Kr and Xe at room temperature, J. Phys. D. Appl. Phys. 48 (46) (2015) 465306.

[11] Z.A.Y. Abdalla, M.Y.A. Ismail, E.G. Njoroge, T.T. Hlatshwayo, E. Wendler, J. B. Malherbe, Migration behaviour of selenium implanted into polycrystalline 3C-SiC, Vacuum 175 (2020), 109235.

[12] Z.A.Y. Abdalla, M.Y.A. Ismail, E.G. Njoroge, E. Wendler, J.B. Malherbe, T.T. Hlatshwayo, Effect of heat treatment on the migration behaviour of selenium implanted into polycrystalline SiC, Nucl. Instrum. Methods Phys. Res., Sect. B 487 (2021) 30-37.

[13] E. Friedland, J.B. Malherbe, N.G. van der Berg, T. Hlatshwayo, A.J. Botha, E. Wendler, W. Wesch, Study of silver diffusion in silicon carbide, J. Nucl. Mater. 389 (2) (2009) 326–331.

[14] K. G¨artner, Modified master equation approach of axial dechanneling in perfect compound crystals, Nucl. Instrum. Methods Phys. Res., Sect. B 227 (4) (2005) 522–530.

[15] J.B. Malherbe, P.A. Selyshchev, O.S. Odutemowo, C.C. Theron, E.G. Njoroge, D. F. Langa, T.T. Hlatshwayo, Diffusion of a mono-energetic implanted species with a Gaussian profile, Nucl. Instrum. Methods Phys. Res. Sect. B Beam Interact. Mater. Atoms 406 (Sep. 2017) 708–713.

[16] G. Litrico, N. Piluso, F. La Via, Detection of crystallographic defects in 3C-SiC by micro-Raman and micro-PL analysis, in: Materials Science Forum, Trans Tech Publications 897 (2017) 303–306.

[17] Z. Xu, Z. He, Y. Song, X. Fu, M. Rommel, X. Luo, A. Hartmaier, J. Zhang, F. Fang, Topic review: application of Raman spectroscopy characterization in micro/nano-machining, Micromachines 9 (7) (2018) 361.

[18] S. Sorieul, J.M. Costantini, L. Gosmain, L. Thomé, J.J. Grob, Raman spectroscopy study of heavy-ion-irradiated α-SiC, J. Phys.: Condens. Matter 18 (22) (2006) 5235.

[19] S. Sanchita, and S. Umapathy, Raman spectroscopy explores molecular structural signatures of hidden materials in depth: Universal Multiple Angle RamanSpectroscopy, Sci. Rep. 4 (2014) 5308.

[20] P. Colomban and A. Slodczyk, Raman intensity: An important tool to study the structure and phase transitions of amorphous/crystalline materials, Optical materials 31 (12) (2009) 1759-1763.

[21] T. Beechem and S. Graham, Temperature and doping dependence of phonon lifetimes and decay pathways in GaN, Journal of Applied Physics 103 (9) (2008) 093507.

[22] Y. Kang, Y. Qiu, Z. Lei, and Hu. Ming, An application of Raman spectroscopy on the measurement of residual stress in porous silicon, Optics and lasers in engineering 43 (8) (2005) 847-855.

[23] B. D. Chalifoux, Y. Yao, K. B. Woller, R. K. Heilmann, and M. L. Schattenburg, Compensating film stress in thin silicon substrates using ion implantation, Optics express 27 (8) (2019) 11182-11195.

[24] S. M. Myers, S. T. Picraux, and T. S. Prevender, Study of Cu diffusion in Be using ion backscattering, Phy. Rev. B 9 (10) (1974) 3953.

[25] A. Benyagoub and A. Audren, Mechanism of the swift heavy ion induced epitaxial recrystallization in predamaged silicon carbide, Journal of Applied Physics 106 (8) (2009) 083516.